Coupled quantized mechanical oscillators

K. R. Brown,* C. Ospelkaus, Y. Colombe, A. C. Wilson, D. Leibfried, and D. J. Wineland
Time and Frequency Division, National Institute of Standards and Technology, 325 Broadway, Boulder, CO 80305, USA

The harmonic oscillator is one of the simplest physical systems but also one of the most fundamental. It is ubiquitous in nature, often serving as an approximation for a more complicated system or as a building block in larger models. Realizations of harmonic oscillators in the quantum regime include electromagnetic fields in a cavity [1–3] and the mechanical modes of a trapped atom [4] or macroscopic solid [5]. Quantized interaction between two motional modes of an individual trapped ion has been achieved by coupling through optical fields [6], and entangled motion of two ions in separate locations has been accomplished indirectly through their internal states [7]. However, direct controllable coupling between quantized mechanical oscillators held in separate locations has not been realized previously. Here we implement such coupling through the mutual Coulomb interaction of two ions held in trapping potentials separated by 40 μm (similar work is reported in a related paper [8]). By tuning the confining wells into resonance, energy is exchanged between the ions at the quantum level, establishing that direct coherent motional coupling is possible for separately trapped ions. The system demonstrates a building block for quantum information processing and quantum simulation. More broadly, this work is a natural precursor to experiments in hybrid quantum systems, such as coupling a trapped ion to a quantized macroscopic mechanical or electrical oscillator [9–13].

The direct coupling of atomic ions in separate potential wells is a key feature of proposals to implement quantum simulation [14–16], and it could allow logic operations to be performed in a multi-zone quantum information processor [10, 17, 18] without the requirement of bringing the ion qubits into the same trapping potential. Moreover, the coupling could prove useful for metrology and sensing. For example, it could extend the capabilities of quantum-logic spectroscopy [9, 19, 20] to ions that cannot be trapped within the same potential well as the measurement ion, such as oppositely charged ions or even anti-matter particles [9, 10]. Coupling could be obtained either through mutually shared electrodes [9, 21] or directly through the Coulomb interaction [10, 17, 22, 23].

The Coulomb interaction potential for two trapped ions, a and b, with charges q_a and q_b in potential wells separated by a distance s_0 is given by

$$\begin{aligned} U(x_a,x_b) &= \frac{1}{4\pi\varepsilon_0}\frac{q_a q_b}{s_0 - x_a + x_b} \\ &\approx \frac{1}{4\pi\varepsilon_0}\frac{q_a q_b}{s_0}\left(1+\frac{x_a-x_b}{s_0}+\frac{x_a^2}{s_0^2}+\frac{x_b^2}{s_0^2}-\frac{2x_a x_b}{s_0^2}\right). \end{aligned}$$

Here x_a and x_b are the displacements of the ions from the external potential minima and ε_0 is the permittivity of free space. The first term is constant and does not affect the dynamics. The second term represents a steady force between the ions that displaces them slightly; if necessary, it can be counteracted with additional potentials applied to nearby electrodes. The terms proportional to x_a^2 and x_b^2 represent static changes in the trap frequencies that could also be compensated with potentials applied to nearby electrodes. The term proportional to $x_a x_b$ represents the lowest-order coupling between the ions' motions. For small deviations, x_a' and x_b', from equilibrium, the coupling is

$$\frac{-q_a q_b}{2\pi\varepsilon_0 s_0^3}(x_a' x_b') = -\hbar\Omega_{\rm ex}(a+a^\dagger)(b+b^\dagger) \approx -\hbar\Omega_{\rm ex}(ab^\dagger + a^\dagger b), \tag{1}$$

where

$$\Omega_{\rm ex} \equiv \frac{q_a q_b}{4\pi\varepsilon_0 s_0^3\sqrt{m_a m_b}\sqrt{\omega_{0a}\omega_{0b}}}, \tag{2}$$

and a, $a^\dagger$, b, and $b^\dagger$ represent the harmonic oscillator lowering (a, b) and raising ($a^\dagger$, $b^\dagger$) operators, m_i and ω_{0i} are respectively the ion masses and motional frequencies, $\hbar$ is Planck's constant divided by 2π, and we have neglected fast-rotating terms. Minimizing the distance, s_0, between ions is crucial, because for fixed ω_{0i}, the coupling rate scales as $\Omega_{\rm ex} \propto 1/s_0^3$.

When $\omega_{0a} = \omega_{0b} = \omega_0$ (the resonance condition), we find

$$\begin{aligned} a^\dagger(t) &= \exp(i\omega_0 t)(a^\dagger(0)\cos(\Omega_{\rm ex}t) - ib^\dagger(0)\sin(\Omega_{\rm ex}t)) \\ b^\dagger(t) &= \exp(i\omega_0 t)(b^\dagger(0)\cos(\Omega_{\rm ex}t) - ia^\dagger(0)\sin(\Omega_{\rm ex}t)). \end{aligned} \tag{3}$$

At time $t = \tau_{\rm ex} \equiv \pi/2\Omega_{\rm ex}$, the operators have changed roles up to a phase factor, and the oscillators have completely swapped their energies, regardless of their initial states. At $t = 2\tau_{\rm ex}$, the energies have returned to their initial values in each ion. The mean occupation, $\langle a^\dagger a\rangle$, of ion a as a function of time exhibits oscillations with period $2\tau_{\rm ex}$.

Figure 1 shows a micrograph of our surface-electrode trap [24], constructed of gold electrodes, 8 μm thick with 5-μm gaps, electroplated onto a crystalline quartz substrate. The trap can produce two potential minima at a height $d_0 = 40$ μm above the surface and separated by $s_0 = 40$ μm along the x axis. Each potential well confines a single $^9Be^+$ ion with an axial (parallel to x) motional frequency of $\omega_0/(2\pi) \approx 4$ MHz and a barrier between wells of ~ 3 meV. Pseudopotential confinement in radial directions (normal to x) is accomplished with a peak potential of ~ 100 V at 170 MHz applied to the radio-frequency electrodes, yielding radial frequencies of ~ 22 MHz. By applying static potentials to the d.c. electrodes, we can independently vary the separation between

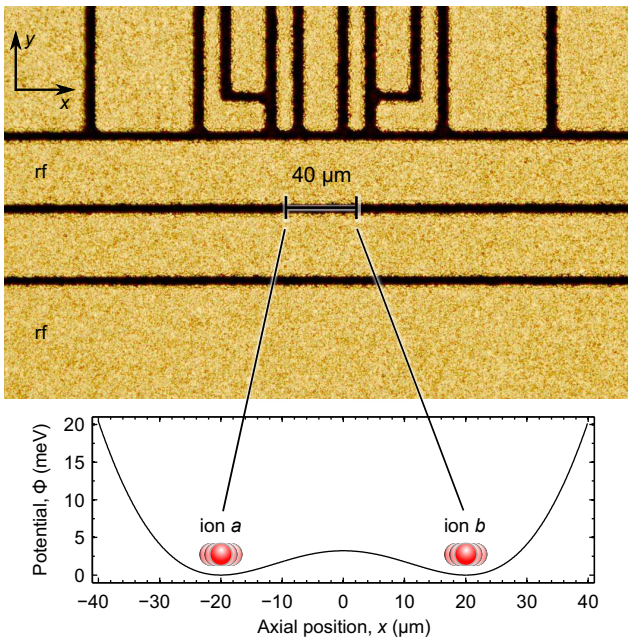

FIG. 1: Micrograph of the ion trap, showing radio-frequency (RF) and d.c. electrodes, and gaps between electrodes (darker areas). The lower part of the figure indicates the simulated potential along the trap x axis. Two trapping wells are separated by 40 μm, with ion positions marked by red spheres. The d.c. electrodes are sufficient to control the axial frequency and the position of each ion independently. Here both frequencies are ~ 4 MHz and the potential barrier between the two ions is ~ 3 meV.

the ions and the curvatures of the two trapping wells. In this way, the ion axial motional frequencies can be brought into or out of resonance, allowing a tunable interaction. For $\omega_0/2\pi = 4.04$ MHz, we predict that $\tau_{ex} = 162$ μs, where we have included a 2% correction in Ω_{ex} owing to the metallic electrodes beneath the ions (Methods Summary).

With currently achieved size scales in ion traps, the Coulomb interaction is relatively weak, so low ion heating rates and stable trapping potentials are essential. Heating rates can be suppressed by operating at cryogenic temperatures [25, 26], so that the direct Coulomb coupling rate can exceed the heating rate. In this work, the trap electrodes and surrounding vacuum enclosure are cooled to 4.2 K with a liquid helium bath cryostat. With similar versions of this trap at $\omega_0/2\pi = 2.3$ MHz, heating rates expressed as $d\langle n\rangle/dt$ (where n denotes the quantum number of motional Fock state $|n\rangle$ and $\langle n\rangle$ is its expectation value) were observed to be as low as 70 quanta per second, consistent with the results of ref. 26. However, for the experiments described here ($\omega_0/2\pi \approx 4.0-5.6$ MHz) the heating rate was $\sim 500-2,000$ quanta per second and varied between the two wells. We observed $d\langle n\rangle/dt \propto 1/\omega_0^2$ in this trap, in agreement with previous reports [25–27], so large values of ω_0 are beneficial. The use of $^9Be^+$, the lightest of the commonly trapped atomic ions, is an advantage here, because for given d.c. trapping potentials the heating rate should remain unchanged while $\Omega_{ex} \propto m^{-1/2}$. Cryogenic operation decreases the background gas pressure to negligible levels, such that ion loss rates due to collisions with background gas are smaller than one per day.

A signature of coupling between the ions is the splitting between the two axial normal mode frequencies. As the trap potential is tuned into the resonance condition, this splitting, δf, reaches a theoretical minimum $\delta f = \Omega_{ex}/\pi = 3.1$ kHz. A plot of the mode frequencies will therefore show an avoided crossing. We measure the mode frequencies by applying a nearly resonant oscillating potential pulse to one of the trap electrodes. We then illuminate both ions with laser radiation resonant with the $^2S_{1/2} - {}^2P_{3/2}$ cycling transition at 313 nm. A decrease in the resulting fluorescence indicates that a mode of the ions' motion has been resonantly excited. For pulse lengths $\tau_p \gg 1/\delta f$, we resolve the two modes (Fig. 2a). We sweep the trapping wells through resonance by varying the static potentials that are applied to the trap electrodes. A plot of the resulting mode frequencies, determined as above, is given in Fig. 2b, c, showing a minimum of $\delta f = 3.0(5)$ kHz, in agreement with theory.

To demonstrate coupling at the level of a few motional quanta, we observe the exchange of energy between the two ions as follows. The ion motional frequencies are initially detuned by 100 kHz, which is much greater than $\Omega_{ex}/(2\pi)$, effectively decoupling the ions' motions. The ions are then simultaneously illuminated with a laser detuned by -10 MHz from the $^2S_{1/2} - {}^2P_{3/2}$ cycling transition, cooling them into a thermal state at the Doppler limit with mean occupation $\langle n\rangle = 2.3(1)$. Subsequently, ion a is cooled to $\langle n_a\rangle = 0.35(2)$ by several cycles of stimulated Raman cooling with the $|\downarrow\rangle \equiv |F = 2, m_F = -2\rangle$ and $|\uparrow\rangle \equiv |1,-1\rangle$ hyperfine states [28]. The Raman beams are counter-propagating and oriented at 45° relative to the x axis. At this point the potentials are brought into resonance ($\omega_0/2\pi = 4.04$ MHz) within an interval (9 μs) short in comparison with τ_{ex} but long in comparison with the axial oscillation period. They remain on resonance for a time τ, allowing energy to transfer between the ions. After a time τ, the potentials are adiabatically returned to their off-resonance values and we determine the mean quantum number, $\langle n_a\rangle$, in ion a by observing asymmetry between the red and blue motional sidebands of the $|\downarrow\rangle$-to-$|\uparrow\rangle$ hyperfine Raman transition [28].

As seen in Fig. 3, energy exchanges between the ions during an interval $\tau_{ex} = 155(1)$ μs. The 5% disagreement between the measured and predicted (162 μs) values for τ_{ex} is probably due to uncertainty in the ion separation, s_0 (even a 1-μm uncertainty would account for the disagreement). The first maximum of $\langle n_a\rangle$ corresponds to the cooling limit of ion b ($\langle n_b(\tau = 0)\rangle = 2.3(1)$ quanta). The underlying linear growth in $\langle n_a\rangle$ corresponds to heating of the ions at a rate of $\dot{\bar{n}} = 1,885(10)$ quanta per second (Methods Summary).

As a final experiment, we demonstrate energy exchange at approximately the single-quantum level. Ideally, the experiment takes the following form. The ions are tuned to the resonance condition throughout and are initially Doppler cooled.

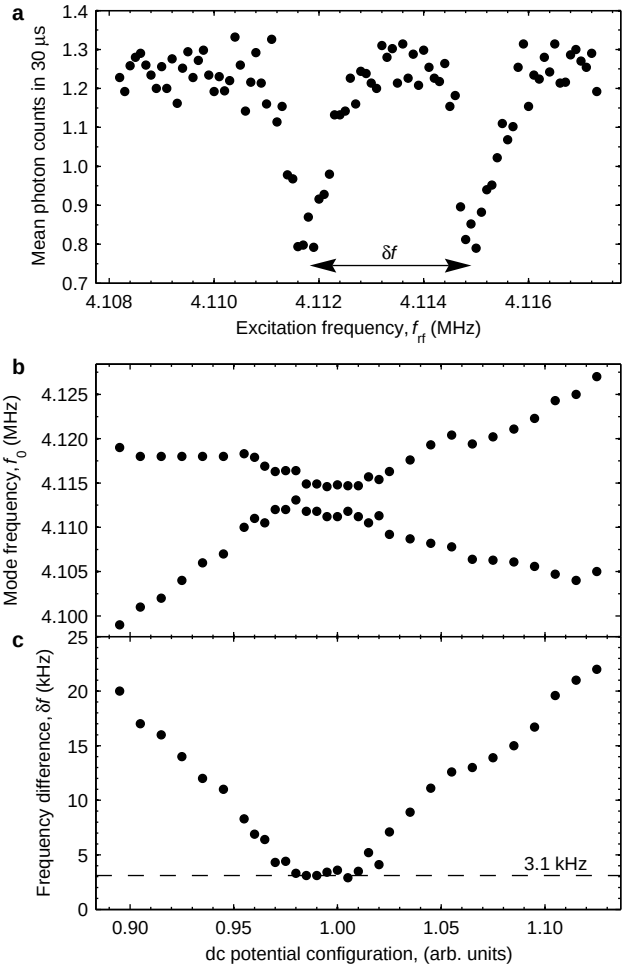

FIG. 2: Motional spectroscopy of two coupled ions near the avoided crossing. **a**, Decreases in collected fluorescence occur at values of excitation frequency, $f_{\rm rf}$, corresponding to the ion mode frequencies. With $\tau_p = 960\ \mu$s, the splitting on resonance is resolved. **b**, **c**, Mode frequencies (**b**) and mode frequency splitting, δf (**c**), for the axial normal modes of two ions separated by 40 μm. Error bars are smaller than the size of the points. The data were acquired over a 1-h period, and slow variations in ambient potentials gave rise to the fluctuations.

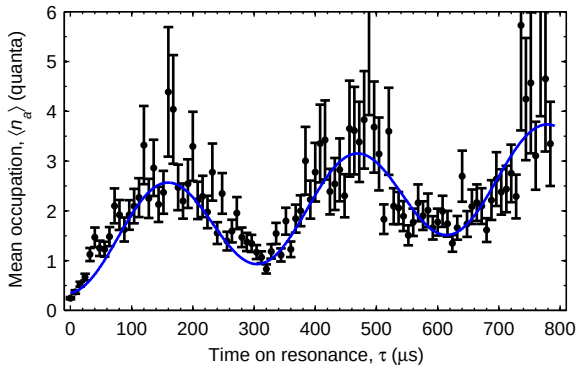

FIG. 3: Energy swapping between two ions in separate trapping potentials at the level of a few quanta. The mean occupation, $\langle n_a \rangle$, of ion a is plotted with error bars (s.e.m.) for various durations, τ, that the ion motional frequencies remain on resonance. The blue curve represents a fit to theory with four free parameters: the two initial mean quantum numbers, the exchange time and the heating rate. Energy exchanges between the ions at 155(1)-μs intervals. The linearly increasing trend in $\langle n_a \rangle$ is due to ion heating at a rate of 1,885(10) quanta per second. Uncertainties represent standard errors of the fit parameters.

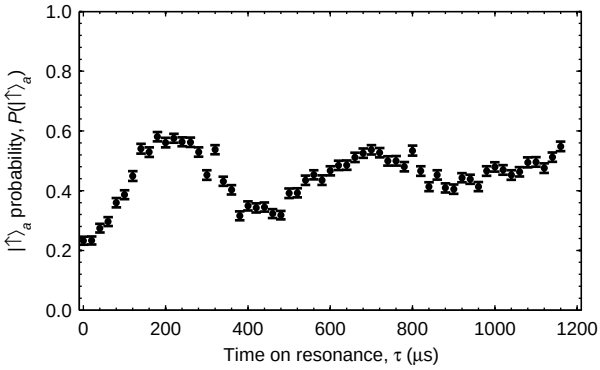

FIG. 4: Motional exchange between two ions in separate trapping potentials at approximately the single-quantum level. The probability, $P(|\uparrow\rangle_a)$, of measuring ion a in spin state $|\uparrow\rangle_a$ at the end of the experimental sequence is plotted with error bars (s.e.m.) against the time, τ, for which the ions interact. $P(|\uparrow\rangle_a)$ oscillates with period $2\tau_{\rm ex} = 437(4)\ \mu$s as a quantum exchanges between the ions.

Ion a is Raman-cooled, sympathetically cooling ion b and thereby preparing the state $|0\rangle_a|\downarrow\rangle_a|0\rangle_b$. To create a single motional quantum, we drive ion a with a blue-sideband Raman π pulse (of duration 10 μs, which is much less than $\tau_{\rm ex}$), creating the state $|1\rangle_a|\uparrow\rangle_a|0\rangle_b$. The system oscillates between $|1\rangle_a|\uparrow\rangle_a|0\rangle_b$ and $|0\rangle_a|\uparrow\rangle_a|1\rangle_b$ with period $2\tau_{\rm ex}$. After a time τ, we drive ion a with another blue-sideband π pulse, conditionally flipping the spin from $|1\rangle_a|\uparrow\rangle_a$ to $|0\rangle_a|\downarrow\rangle_a$, dependent on the presence of a motional quantum in ion a. The final internal state probability will be given by $P(|\uparrow\rangle_a)(\tau) = \sin^2(\Omega_{\rm ex}\tau)$. In practice, contrast in the oscillations (Fig. 4) is significantly reduced by incomplete cooling, motional decoherence and decoherence due to imperfect Raman sideband pulses. We estimate that ion a is cooled initially to $\langle n_a \rangle = 0.3(1)$. Although we were unable to measure the initial temperature of ion b directly, comparison of the contrast and temporal behavior of our exchange data (Fig. 4) with simulations indicates that $\langle n_b \rangle \lesssim 0.6$. Motional decoherence results from heating and from trap frequency instability over the time required to acquire the data. Raman sideband pulses suffer from variations in laser intensity and fluctuations in the sideband coupling caused by thermal spread in the y and z motional states (Debye-Waller factors [10]). For $\omega_0/2\pi = 5.56$ MHz, we observe oscillations with period $2\tau_{\rm ex} = 437(4)\ \mu$s. The 2% disagreement with the prediction (447 μs) of equations 2 and 3 is probably due to uncertainty in the ion separation and the difficulty of maintaining the exact resonance condition.

Significant improvements in coupling fidelity seem to be in reach with current technology. It should be possible to improve Raman laser intensity stability, and Debye-Waller factors from the y and z motion can be eliminated by proper choice of beam directions [28]. We believe that our motional frequency instability can be alleviated by ensuring that the trap surface is free of charged contaminants. Faster exchange can be achieved by scaling down trap dimensions, but this puts a premium on reduced motional heating. Although the work presented here uses the axial mode to couple the ions, it may prove advantageous to use the radial modes in future experiments because of the lower heating rates associated with their higher frequencies. As an example, radial mode frequencies of ~ 30 MHz are routinely achieved in the apparatus, compared with axial frequencies $\lesssim 10$ MHz.

These results could lead to several possible applications in quantum state engineering and spectroscopy. For example, from the motional state $|1\rangle_a|0\rangle_b$ the state of the ions at time $t = \tau_{\rm ex}/2$ is the Bell state $(|1\rangle_a|0\rangle_b + i|0\rangle_a|1\rangle_b)/\sqrt{2}$. Transferring this state onto the ions' internal states with sideband pulses would create an entangled spin state, even between ions of dissimilar species. This could be used as an entangled-pair factory in the scheme of refs 10,18, with the advantage over previous schemes [7] that the ions are already in separate wells, ready for distribution to separate locations. The coupling could be used to read out the state of one ion species with another, an ability useful for error correction protocols and for quantum logic spectroscopy [19]. When the harmonic wells are not in resonance, the spin state of one ion can be read out without destroying the state of the other, so schemes for weak or quantum non-demolition measurements that use either Kerr-type nonlinearities or quantum logic may become feasible [1]. Hybrid quantum systems, incorporating similar interactions to couple a trapped ion to other quantum devices, could serve as a means of transferring quantum information between different qubit implementations in a future quantum network. For example, a trapped ion could act as a quantum transformer between a superconducting qubit [13] and a photonic qubit [29, 30]. The sympathetic cooling through exchange might also be used to cool neutral molecules [31].

METHODS SUMMARY

The shielding factor, β, represents the ratio of the exchange rates $\Omega_{\rm ex}$ with and without the presence of the trapping electrodes. To a good approximation, we ensure that at the motional frequencies all trap electrodes are held at ground. Therefore, assuming that gaps between the electrodes are negligible, the shielding factor can be calculated with the method of images. The result is

$$\beta = 1 - \frac{1}{2}\left(\frac{3(s_0/d_0)^5}{(4+(s_0/d_0)^2)^{5/2}} - \frac{(s_0/d_0)^3}{(4+(s_0/d_0)^2)^{3/2}}\right) \quad (4)$$

which reaches a maximum of $\beta = 1.018$ at $s_0 = d_0$.

The evolution of $\langle n_a\rangle$ under the influence of equation 1, including heating effects and assuming that both ions begin in a thermal state with mean quantum numbers n_{a0} and n_{b0}, can be predicted with a Langevin equation [9]. On resonance, the evolution is

$$\langle n_a\rangle = n_{a0}\cos^2(\Omega_{\rm ex}t) + n_{b0}\sin^2(\Omega_{\rm ex}t) + \dot{\bar{n}}t \quad (5)$$

where $\dot{\bar{n}}$ represents the mean of $d\langle n_a\rangle/dt$ and $d\langle n_b\rangle/dt$ for uncorrelated noise sources.

* Electronic address: kenton.brown@nist.gov

[1] Haroche, S. & Raimond, J.-M. *Exploring the Quantum: Atoms, Cavities, and Photons* (Oxford Univ. Press, 2006).

[2] Miller, R. *et al.* Trapped atoms in cavity QED: coupling quantized light and matter. *J. Phys. B* **38**, S551 (2005).

[3] Houck, A. A. *et al.* Generating single microwave photons in a circuit. *Nature* **449**, 328–331 (2007).

[4] Leibfried, D., Blatt, R., Monroe, C. & Wineland, D. J. Quantum dynamics of single trapped ions. *Rev. Mod. Phys.* **75**, 281–324 (2003).

[5] O'Connell, A. D. *et al.* Quantum ground state and single-phonon control of a mechanical resonator. *Nature* **464**, 697–703 (2010).

[6] Monroe, C. *et al.* Scalable entanglement of trapped ions. In Arimondo, E., De Natale, P. & Inguscio, M. (eds.) *Atomic Physics 17, Proceedings of the 17th International Conference*, 173–186 (2001).

[7] Jost, J. D. *et al.* Entangled mechanical oscillators. *Nature* **459**, 683–685 (2009).

[8] Harlander, M., Lechner, R., Brownnutt, M., Blatt, R. & Hänsel, W. Trapped-ion antennae for the transmission of quantum information. *Nature* **471**, 200–203 (2011).

[9] Heinzen, D. J. & Wineland, D. J. Quantum-limited cooling and detection of radio-frequency oscillations by laser-cooled ions. *Phys. Rev. A* **42**, 2977–2994 (1990).

[10] Wineland, D. J. *et al.* Experimental issues in coherent quantum-state manipulation of trapped atomic ions. *J. Res. Nat. Inst. Stand. Tech.* **103**, 259–328 (1998).

[11] Tian, L. & Zoller, P. Coupled ion-nanomechanical systems. *Phys. Rev. Lett.* **93**, 266403 (2004).

[12] Hensinger, W. K. *et al.* Ion trap transducers for quantum electromechanical oscillators. *Phys. Rev. A* **72**, 041405(R) (2005).

[13] Tian, L., Blatt, R. & Zoller, P. Scalable ion trap quantum computing without moving ions. *Eur. Phys. J. D* **32**, 201–208 (2005).

[14] Schmied, R., Roscilde, T., Murg, V., Porras, D. & Cirac, J. I. Quantum phases of trapped ions in an optical lattice. *New J. Phys.* **10**, 045017 (2008).

[15] Chiaverini, J. & Lybarger, Jr., W. E. Laserless trapped-ion quantum simulations without spontaneous scattering using microtrap arrays. *Phys. Rev. A* **77**, 022324 (2008).

[16] Schmied, R., Wesenberg, J. H. & Leibfried, D. Optimal surface-electrode trap lattices for quantum simulation with trapped ions. *Phys. Rev. Lett.* **102**, 233002 (2009).

[17] Cirac, J. I. & Zoller, P. A scalable quantum computer with ions in an array of microtraps. *Nature* **404**, 579–581 (2000).

[18] Kielpinski, D., Monroe, C. & Wineland, D. J. Architecture for a large-scale ion-trap quantum computer. *Nature* **417**, 709–711 (2002).

[19] Schmidt, P. O. *et al.* Spectroscopy using quantum logic. *Science* **309**, 749–752 (2005).

[20] Rosenband, T. *et al.* Frequency ratio of Al^+ and Hg^+ single-ion optical clocks; metrology at the 17th decimal place. *Science* **319**, 1808–1812 (2008).
[21] Daniilidis, N., Lee, T., Clark, R., Narayanan, S. & Häffner, H. Wiring up trapped ions to study aspects of quantum information. *J. Phys. B* **42**, 154012 (2009).
[22] Tan, J. N. Interacting ion oscillators in contiguous confinement wells. *Bull. Am. Phys. Soc.* **47**, 103 (2002).
[23] Ciaramicoli, G., Marzoli, I. & Tombesi, P. Scalable quantum processor with trapped electrons. *Phys. Rev. Lett.* **91**, 017901 (2003).
[24] Seidelin, S. *et al.* Microfabricated surface-electrode ion trap for scalable quantum information processing. *Phys. Rev. Lett.* **96**, 253003 (2006).
[25] Deslauriers, L. *et al.* Scaling and suppression of anomalous heating in ion traps. *Phys. Rev. Lett.* **97**, 103007 (2006).
[26] Labaziewicz, J. *et al.* Temperature dependence of electric field noise above gold surfaces. *Phys. Rev. Lett.* **101**, 180602 (2008).
[27] Epstein, R. J. *et al.* Simplified motional heating rate measurements of trapped ions. *Phys. Rev. A* **76**, 033411 (2007).
[28] Monroe, C. *et al.* Resolved-sideband Raman cooling of a bound atom to the 3D zero-point energy. *Phys. Rev. Lett.* **75**, 4011–4014 (1995).
[29] Cirac, J. I., Zoller, P., Kimble, H. J. & Mabuchi, H. Quantum state transfer and entanglement distribution among distant nodes in a quantum network. *Phys. Rev. Lett.* **78**, 3221–3224 (1997).
[30] Moehring, D. L. *et al.* Entanglement of single-atom quantum bits at a distance. *Nature* **449**, 68–71 (2007).
[31] Idziaszek, Z., Calarco, T. & Zoller, P. Ion-assisted ground-state cooling of a trapped polar molecule. *http://arxiv.org/abs/1008.1858* (2010).

Acknowledgements This work was supported by IARPA, DARPA, ONR and the NIST Quantum Information Program. We thank M. Biercuk, A. VanDevender, J. Amini, and R. B. Blakestad for their help in assembling parts of the experiment, and we thank U. Warring and R. Simmonds for comments. This paper, a submission of NIST, is not subject to US copyright.

Author Contributions K.R.B. and C.O. participated in the design of the experiment and built the experimental apparatus. K.R.B. collected data, analysed results and wrote the manuscript. Y.C. fabricated the ion trap chip and collected data. A.C.W. maintained laser systems and collected data. D.L. participated in the design of the experiment, collected data and maintained laser systems. D.J.W. participated in the design and analysis of the experiment. All authors discussed the results and the text of the manuscript.

Author Information Reprints and permissions information is available at www.nature.com/reprints. The authors declare no competing financial interests. Readers are welcome to comment on the online version of this article at www.nature.com/nature. Correspondence and requests for materials should be addressed to K.R.B. (kenton.brown@nist.gov).